25th ABCM International Congress of Mechanical Engineering
October 20-25, 2019, Uberlândia, MG, Brazil

# COB-2019-1881
# THERMODYNAMIC ANALYSIS OF ADIABATIC EXTERNAL COMBUSTION ENGINE

**Silvio Cesar Dalmolin**
**Matias Nicolas Muñoz**
Graduate Program in Mechanical Engineering – PGMEC, Federal University of Parana – UFPR, Av. Cel. Francisco H. dos Santos, 100 - Jardim das Americas, Curitiba - PR, Brazil.
scdalmolin@gmail.com
matiasmunuoz@gmal.com

**José Viriato Coelho Vargas**
Mechanical Engineering Department – DEMEC, Federal University of Parana – UFPR, Av. Cel. Francisco H. dos Santos, 100 - Jardim das Americas, Curitiba - PR, Brazil.
vargasjvcv2@gmail.com

***Abstract.*** *Thermodynamic analysis of a combustion engine with external and adiabatic combustion chamber (EACE) is accomplished. The admission and compression strokes happen in separated cylinders from expansion and exhaust; In addition, the combustion carry out in an external and adiabatic fixed volume chamber; Inside the chamber, because the combustion heat input, occurs an isochoric compression with increasing pressure and temperature, similar that occurs in the Carnot cycle; The EACE has five strokes. A comparative thermodynamic analysis between a market compression ignition combustion engine (IC-ICE) and an EACE, with same volumetric displacement, is carry out. The thermal performance of machines are evaluated through a simplified mathematical model; Moreover, the mass and energy balances are calculated; the thermal efficiency of the new proposed motor is around 45 %; Being greater than conventional chosen engine, that is only 34 %.*

***Keywords:*** *External combustion engine, adiabatic engine, internal combustion engine, thermodynamic analysis.*

## 1. INTRODUCTION

The ignited compression internal combustion engine (IC-ICE), also known as diesel engine, because it is versatility, performance, efficiency and other characteristics, it is one of the most used thermal machines in the world. The German engineer Rudolf Diesel patented it in 1892. At 1893, he have published his famous dissertation: "Theory and Construction of a Rational Heat-engine to replace the Steam Engine and The Combustion Engines Known Today".

IC-ICE is used in several applications, like vehicles and trucks driven, thermal power plants, as stand by power in critical applications, isolated power in remote places, vessels, locomotives and so on.

Figure 1, taken from Moran and Shapiro (2000), shows the *P*-*V* (pressure versus volume) and *T*-*s* (temperature versus entropy) diagrams of the ideal diesel cycle. They show the four process or strokes: stroke 1-2 isentropic compression; stroke 2-3 heat addition at constant pressure (isobaric); stroke 3-4 isentropic expansion; stroke 4-1 heat rejection at constant volume.

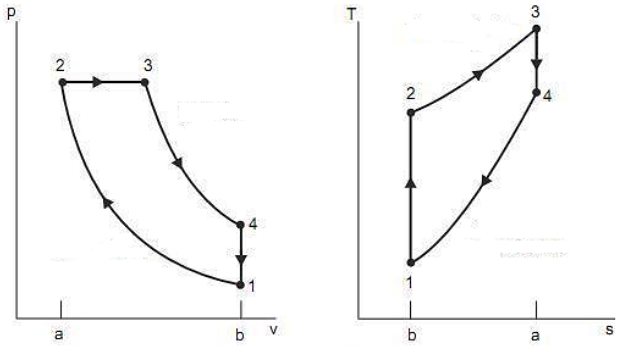


Figure 1. Ideal diesel cycle $P \times V$ and $T \times s$ diagrams. From: Moran and Shapiro (2000)

However, because of the practical limitation, is very difficult to achieve the ideal diesel cycle, even today. Numerous efforts have already done but there are many irreversibility hard to be reduced.

### 1.1 First Law Balance

According to Li, Caton and Jacobs (2016), nowadays, because several economic and environmental factors, there is the necessity to improve the rate of heat to work conversion. Only one-third of the total input heat is converted in useful work in a modern IC-ICE. Most of the input heat is discharged by the exhaust gas and by the engine cooling fluid. The authors have studied an engine with a thermal barrier around the cylinder surface. Also known as low heat rejection engine (LHRE). According to them, the idea is to reduce the thermal losses to the coolant stream and, in this way, improve the amount of heat converted in useful work. It was very studied in the 80's by Cummins Company for instance.

According to Adler and Bandhauer (2017), the energy balance of a typical automotive IC-ICE is showed in Fig. 2. Note that most of the chemical energy from the fuel is rejected by the exhaust stream and by the coolant stream. In addition, the coolant stream has a very low temperature (about 90 ºC) but the exhaust stream has a high temperature (about 400 ºC); i.e., high exergy, so, much useful work can be still taken out from it.

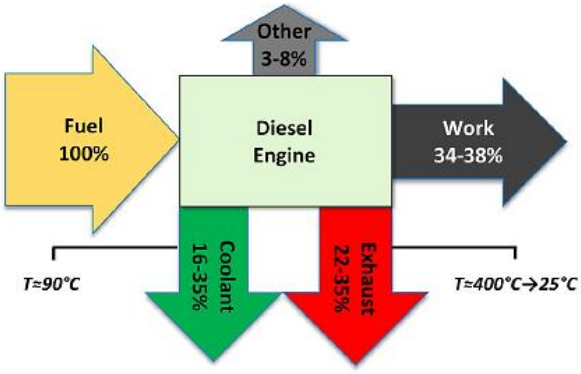


Figure 2. Typical heat balance of an automotive IC-ICE. From: Adler and Bandhauer (2017)

According to Liu et al. (2018), big and moderns IC-ICE shows better efficiency. Although, a maximum thermal efficiency reached in the last generation engine is limited by 50 % and the improvements need to across this barrier are, actually, a challenge. Many strategies were already used to improve thermal efficiency. The authors have done a mathematical model of an internal combustion engine which one shows that the fuel energy converted in useful work growths with the increasing of the thermal barrier in the combustion chamber.

### 1.2 Carnot and Stirling cycles

Since the beginning of the development of modern thermodynamics and the thermal machines, there is an effort to reach the Carnot cycle efficiency. The Carnot cycle is composed of two isochoric and two isothermal processes; it permits the maximum theoretical efficiency according to thermodynamics principals. Therefore, a way to improve IC-ICE efficiency is to approximate it to the Carnot cycle.

The cycles Stirling, Joule, and Ericsson have this objective, each one with some particularity. These particularities do not allow a wide range of use and production.

From the cycles above, the most similar to the Carnot cycle is the Stirling cycle. It works in a closed volume system, with working fluid compression and expansion at different temperatures. The cycle consists of four processes according to $P \times V$ and $T \times s$ diagrams show in Fig. 3. Note they are very similar to Carnot cycle.

In the conventional internal combustion engine (ICE), a great part of the work takes from the expansion stroke is used at compression process. The process 2-3 at the Stirling cycle is an isochoric compression, constant volume, which one does not need work addition. Therefore, possible useful work is bigger. This mechanism is also present at Carnot Cycle. Then, it is possible to conclude the isochoric compression has a great potential to improve the efficiency of the IC-ICEs.

Besides that, as this process occurs in a chamber at constant volume, without the necessity of movable parts, the possibilities to apply the thermal barrier to avoid the heat losses are more simple and easy. Then, not only could the isochoric compression be applied, but also the thermal barrier.

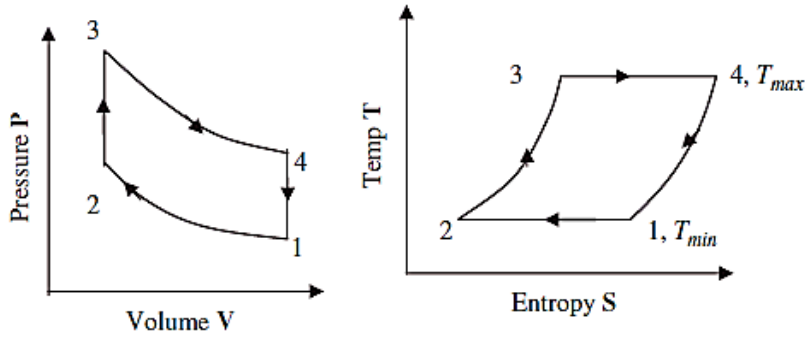


Figure 3. $P \times V$ and $T \times s$ Stirling diagrams. From: Thombare e Verma (2008).

### 1.3 Objectives

Introduce and analyze an external and adiabatic combustion engine (EACE) with a new thermodynamic cycle. The EACE has an additional process when compared with the currently IC-ICE, the external and adiabatic combustion stroke. The main objective is to reach greater performance and efficiency. A new kinematic arrangement mechanism allows the addition of the new stroke is developed. The mathematical simulation is used as a tool to simulate an EACE engine and compare it with an IC-ICE, both with similar size and parameters.

## 2. EACE THERMODINAMIC CYCLE

The EACE engine has a thermodynamic cycle based in the Rudolf Diesel cycle. However, the combustion occurs in an external and adiabatic chamber. At same way than an IC-ICE, an assemblage of pistons connected to a crankshaft composes the EACE. Each piston is inside of a cylinder. Inside the cylinder happens the expansion or the compression process of the working fluid. The expansion and compression strokes take place in different cylinders, not at the same as ICE. Figure 4 shows the working fluid flow schematic inside the EACE and the combustion chamber position in the relationship of the other strokes

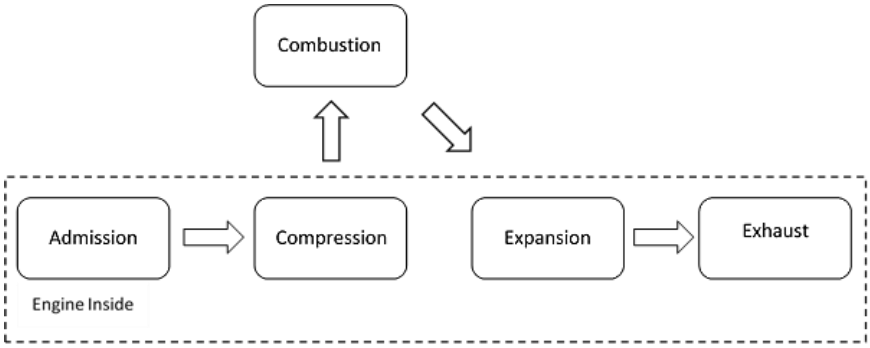


Figure 4. EACE working fluid flow schematic. From: author.

In an IC-ICE the combustion process happening at the beginning of the expansion stroke. Compression and expansion strokes happens at the same cylinder. In the other way, the combustion has a specific place in an EACE, separated from the engine cylinders. The piston admits and compresses the working fluid in a cylinder. After that, it goes to the external combustion chamber, where it is burned together with the fuel. Next, to that, it is sent to other cylinders, which one the expansion and exhaust occur.

The combustion occurs in an external chamber without volume variation. The isochoric compression occurs with the heat addition only, increasing expressively the pressure and temperature.

The combustion process represents an additional stroke when compared with traditional IC-ICE. It needs to start at 360º of crankshaft angle before expansion stroke and immediately after compression stroke. To coupling the external combustion stroke, a new kinematic arrangement is developed. Figure 5 shows the mechanism. The blue region corresponds to a complete EACE cycle.

Note the EACE mechanism: the compression and the expansion stroke are not in the same phase. To solve that, two combustion chambers are fit between compression and expansion strokes. The operation of the two chambers changes one by other each 360º of crankshaft angle. The empty area of combustion chamber corresponds to the filling phase and the hatched area to the burning phase.

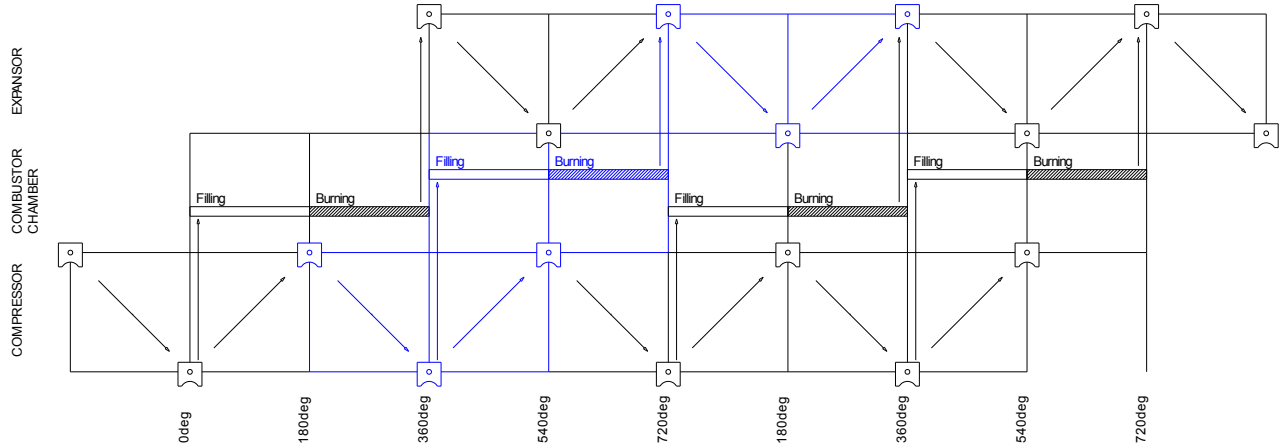


Figure 5. EACE kinematic mechanism. From: Author.

Figure 6 shows an IC-ICE top cylinder and head section view. Note the dead volume in the top of Piston. In the EACE the combustion does not occur anymore inside the cylinder. Consequently, this volume is no more necessary and the dead volume inside the cylinder could be smaller.

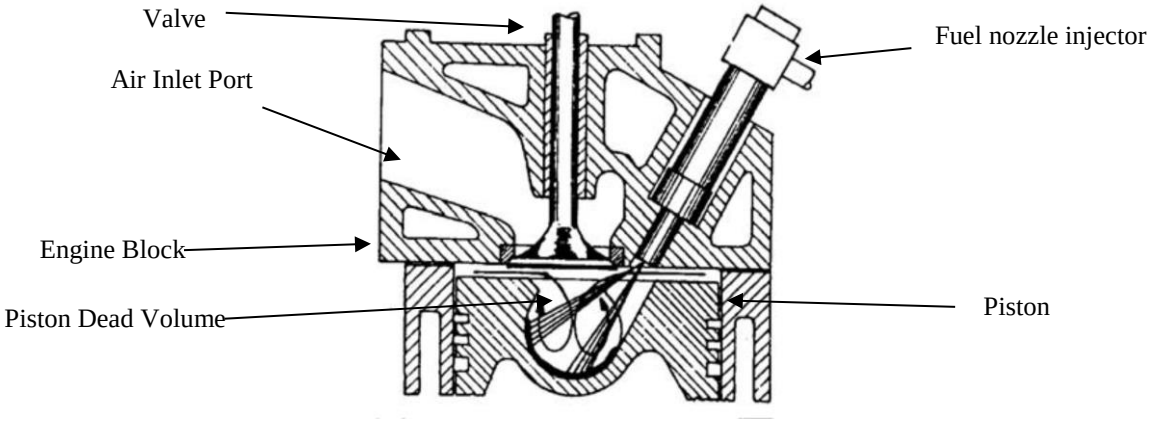


Figure 6. ICE top cylinder and head section view. Adapted from: Santos (2004).

On the other hand, in the EACE exist the volume of the combustion chamber and the piping to connect it to compression and expansion cylinders. To compensate for the necessity of these new volumes, the combustion chamber and connection piping volumes are considered equivalent to piston dead volume. A detailed EACE dead volume analyses must be done in a future study.

The combustion chamber does not need movable parts. Therefore, it can be built of ceramic, for instance.

Besides that, the EACE combustion time is longer than IC-ICE. In the EACE, the combustion process takes 360º of crankshaft angle. There is more time for the combustion process. It can burn better than IC-ICE becoming possible the use of more complex fuels like heavy oils. In addition, it can improve the burning process of biodiesel, for instance.

## 3. MATHEMATICAL MODEL

A conventional IC-ICE and an EACE are modeled. Both them with the same size, same geometric parameters, and same real air to fuel ratio ($AFR_{real}$). The mathematical models of each stroke: admission, compression, combustion, expansion and exhaust, are presented below. The admission, compression e exhaust stroke have the same mathematical model for both cycles. The model of these strokes is based on the work of Graciano (2012).

Only the EACE has the external and adiabatic combustion stroke. In the IC-ICE the combustion occurs inside the expansion stroke while in the EACE exist only working fluid expansion.

Figure 7 shows the crankshaft and rod mechanism working inside the cylinder. The figure also shows the working space of the admission, compression, expansion and exhaust strokes. It is used in these mathematical models. $H_{cyl}$ represents the position of the piston relative to the top of the cylinder, m; *AV* admission valve; *EV* exhaust valve; *TDC* top dead center; *BDC* bottom dead center; *ROD* connecting rod length, m; *CS* crankshaft radius, m (note that it's two times the piston stroke/piston displacement); $\theta$ crankshaft angle position, º (degrees).

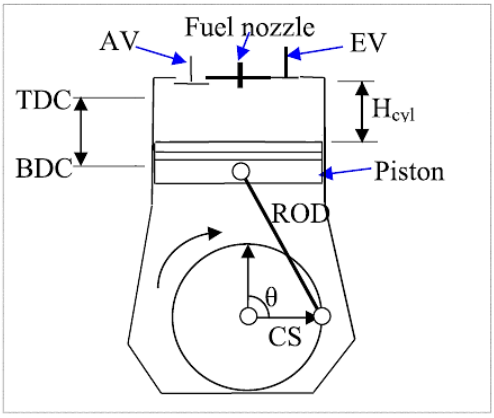


Figure 7. Crankshaft and rod mechanism working inside the cylinder. Adapted from: Graciano (2012).

The mathematical model is divided into several routines. One routine for each stroke.
The equation below represents the instantaneous energy balance. Evaluated for all strokes.

$$\frac{dE_{vc}}{dt} = \frac{dQ_{fuel}}{dt} + \frac{dQ_{lost}}{dt} + \frac{dEh}{dt} - \frac{dW}{dt} \tag{1}$$

$E_{vc}$ represents internal energy of the working fluid, J; $Q_{comb}$ heat released by the combustion process to the working fluid, J; Eh working fluid enthalpy incoming to or leaving the working space, J.
$W$ represents the work done by or to working fluid, in J. Evaluated for all strokes except for EACE combustion stroke.

$$\frac{dW}{dt} = \frac{\pi \cdot Piston_{dia}{}^2}{4} \cdot \frac{d(P \cdot SP)}{dt} \tag{2}$$

Where $P$ represents the working fluid Pressure, in N m$^{-2}$; $t$ is the time, s; $Piston_{dia}$ diameter of the piston, m; $SP$ instantaneous pistons speed, m s$^{-1}$, given by $SP = \frac{dH_{cyl}}{dt}$.
$Q_{lost}$ is the heat lost to the coolant stream trough the cylinders walls, in J. Evaluated for all strokes except for EACE combustion stroke.

$$\frac{dQ_{lost}}{dt} = U_{global} \cdot A_{cyl} \cdot (T - T_w) \tag{4}$$

Where $A_{cyl}$ represents the instantaneous cylinder surface exposed the working fluid, m$^2$; $U_{global}$ heat transfer coefficient, W m$^{-2}$ K$^{-1}$; $T_w$ coolant temperature, K; $T$ working fluid temperature, K.
The instantaneous position of the piston relative to the top of the cylinder is given by equation below.

$$H_{cyl} = ROD + CS \cdot (1 - \cos(\theta)) - \sqrt{ROD^2 - CS^2 \cdot \sin(\theta)^2} \tag{5}$$

The working fluid specific volume, in m$^3$ kg$^{-1}$, is given below. Evaluated for all strokes.

$$\upsilon = \frac{V}{m} \tag{6}$$

Where $m$ represents the instantaneous working fluid mass, kg. $V$ is instantaneous working fluid volume, in m$^3$, given by $V = \pi \cdot \frac{Piston_{dia}^2}{4} \cdot H$. The specific internal energy, in J kg$^{-1}$, is given below. Evaluated for all strokes.

$$\mu = \frac{E_{vc}}{m} \tag{7}$$

From $\upsilon$ and $\mu$, all the other properties are taken from the equation of state.
The compression engine ratio is given by $CR = \frac{H_{max}}{H_{min}}$.
The mathematical model was developed with the following assumptions:

All the thermodynamic parameters like, temperature, pressure, internal energy, and others are uniform inside the working space; the working fluid potential energy and kinetic energy variations are neglected with respect to internal energy variation; dry air with real gas behavior is assumed for the working fluid mixture (reactants and products); all the reactants are consumed in the combustion process (completed combustion). All thermodynamic properties are taken from fundamental equation of state developed by E.W Lemmon (2000) which is implemented in EES Software®. All the equations are evaluated instantaneously at each mathematical model interaction.

### 3.1 Admission stroke and Exhaust Stroke

The working space is treated as an open system. The mass flow, in kg $s^{-1}$, incoming the cylinder is given by:

$$\frac{dm}{dt} = n \cdot C_d \cdot A_{min} \cdot \sqrt{|2 \cdot \rho \cdot (P_{atm} - P)|} \tag{8}$$

Where $A_{min}$ represents the minimum opening admission or exhaust valve area; $\rho$ working fluid density, in kg $m^{-3}$, which one is incoming to or leaving from working space; $C_d$ is the discharge or admission valve coefficient; $n$ is (-1) for exhaust stroke and (1) for admission stroke.

At admission: the admission valve is opened and air incoming the cylinder. The exhaust valve is closed.

At exhaust: the exhaust valve is opened and the air leaving the cylinder. The admission valve is closed.

### 3.2 Compression stroke

The admission and exhaust valve is closed. The working space is treated as a closed system, so m is constant.

### 3.3 EACE combustion stroke

This stroke occurs in the external and adiabatic combustion chamber. The admission and exhaust valve is closed. There is the fuel injection in the chamber but the mass and enthalpy of this stream are very small comparing with working fluid internal energy and mass. Therefore, the working space is treated as a closed system.

The working fluid mass is the sum of the air mass with the fuel mass, given by:

$$\frac{dm}{dt} = \frac{dm_{ar}}{dt} + \frac{dm_{fuel}}{dt} \tag{9}$$

Where $\frac{dm_{fuel}}{dt}$ represents the fuel mass rate incoming the working space, it given by:

$$\frac{dm_{fuel}}{dt} = \frac{dm_{fuel}}{dt} \cdot \frac{1}{AFR_{real}} \tag{10}$$

Where $AFR_{real}$ is the effective combustion mass to fuel ratio, given by $AFR_{real} = AFR_{sch} \cdot \gamma$. $AFR_{sch}$ is the stoichiometric combustion mass to fuel ratio and $\gamma$ is the combustion air excess.

Thermal power released by the combustion process is given below; $W$. $LHV$ represents fuel low heat value, in J $kg^{-1}$.

$$\dot{Q}_{fuel} = LHV \cdot \frac{dm_{fuel}}{dt} \tag{11}$$

### 3.4 Expansion stroke

The admission and exhaust valve is closed. At IC-ICE, there is the fuel injection in the chamber but the mass and enthalpy of this stream are very small comparing with working fluid internal energy and mass. Therefore, the working space is treated as a closed system and m is constant for IC-ICE and EACE. Equation **(**10**)** gives $\dot{m}_{fuel}$, which incoming the working space. Equation (11) gives the heat released by the combustion process. However, all the fuel mass is injected between the beginning of the stroke and the combustion span crankshaft angle, $\Delta\psi$.

### 3.5 Loses by friction and auxliliaries drive

Equation **(**12**)** gives the work consumed to drive auxiliaries and the friction losses:

$$W_{friction} = \overline{P_{fr}} \cdot V_{displaced} \tag{12}$$

Where $\overline{P_{fr}}$ is given by $\overline{P_{fr}} = C1 + C2 \cdot rpm$. Constants $C1$ and $C2$ are adjustable coefficients. rpm represents the crankshaft angular speed, in revolutions per minute. $V_{displaced}$ is given by $V_{displaced} = \pi \cdot \frac{Piston_{dia}^2}{4} \cdot (H_{max} - H_{min})$. Where $H_{min}$ is the $H_{cyl}$ when the piston is in $TDC$ position, in m. $H_{max}$, in m, is given by $H_{max} = H_{min} + 2 \cdot CS$.

### 3.6 Engine Output Variables

Equation (13**)** gives the useful work produce by the engine at each cycle:

$$W_{net} = W_{expansion} - W_{admission} - W_{compression} - W_{exhaust} - W_{friction} \tag{13}$$

$W_{expansion}$ represents the work produced by the expansion stroke, J; $W_{admission}$ the work consumed by the admission stroke, J; $W_{compression}$ the work consumed by the compression stroke, J; $W_{exhaust}$ the work consumed by the exhaust stroke, J.

The total useful power available, in W, at crankshaft is:

$$\dot{W}_{tot} = \frac{W_{net}}{\delta t_{cycle}} \cdot N_{cyl} \tag{14}$$

Where $N_{cyl}$ represents the number of engine cylinders. $\delta t_{cycle}$ is the complete cycle time, in s, given by $\delta t_{cycle} = \frac{120}{rpm}$.

The thermal efficiency is $\eta = \frac{\dot{W}_{tot}}{\dot{Q}in_{tot}}$. $\dot{Q}in_{tot}$ represents the total thermal power, in W, released by the combustion process of all cylinders, given by $\dot{Q}in_{tot} = \dot{Q}_{fuel} \cdot N_{cyl}$.

## 4. MATHEMATICAL MODEL VALIDATION

To demonstrate the accuracy of the mathematical model, a conventional IC-ICE is simulated. The results are compared with experimental data. Lindec 4LD2500 engine from Agrale manufacturer is chosen. The atmospheric pressure considered, $P_{atm}$, is $1{,}013 \times 10^5$ N m$^{-2}$ and the atmospheric temperature considered, $T_{atm}$, is 298,15 K. The mathematical model was evaluated using a second-order predictor-corrector algorithm implemented in EES Software®, version 9.

The input parameters used in mathematical simulation are: $CR$ = 18; $Piston_{dia}$ = 90 × 10$^{-3}$ m; $CS$ = 52,5 × 10$^{-3}$ m; $ROD$ = 192 × 10$^{-3}$ m; $C_d$ = 0,9; $d_{valve}$ = 17,5 × 10$^{-3}$ m; $LHV$ = 42475 × 10$^3$ J kg$^{-1}$; $\lambda$ = 1,4116; $AFR_{sch}$ = 14,7; $T_w$ = 373,15 K; $U_{global}$ = 680 W m$^{-2}$ K$^{-1}$; $\Delta\psi$ = 50 º; $N_{cyl}$ = 4.

Figure 9 shows the $\dot{W}_{tot} \times rpm$ and $\eta \times rpm$ diagrams. The simulated data are compared with experimental data from Pereira HR (2006). The $\eta$ is calculated from the experimental fuel consumption. The error found between experimental and simulated data is smaller than 3 % for $\dot{W}$ and smaller than 7 % for $\eta$. Figure 10 shows $T \times \theta$ diagram at 2800 rpm taken from mathematical model simulation.

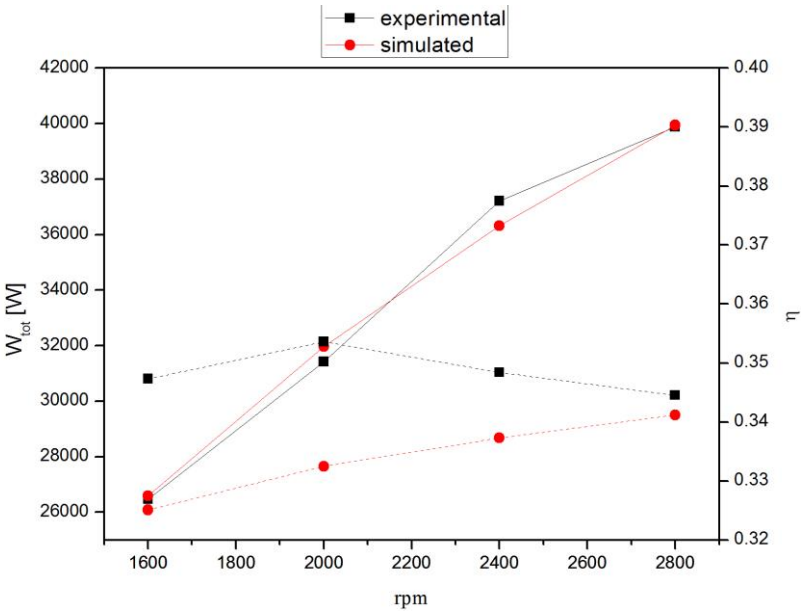


Figure 9. Lindec 4LD2500 $\dot{W}_{tot} \times rpm$ and $\eta \times rpm$ diagram comparative between the mathematical model and experimental data. $\eta$ in dashed lines. Simulated data from: author. Experimental data from: Pereira HR (2006).

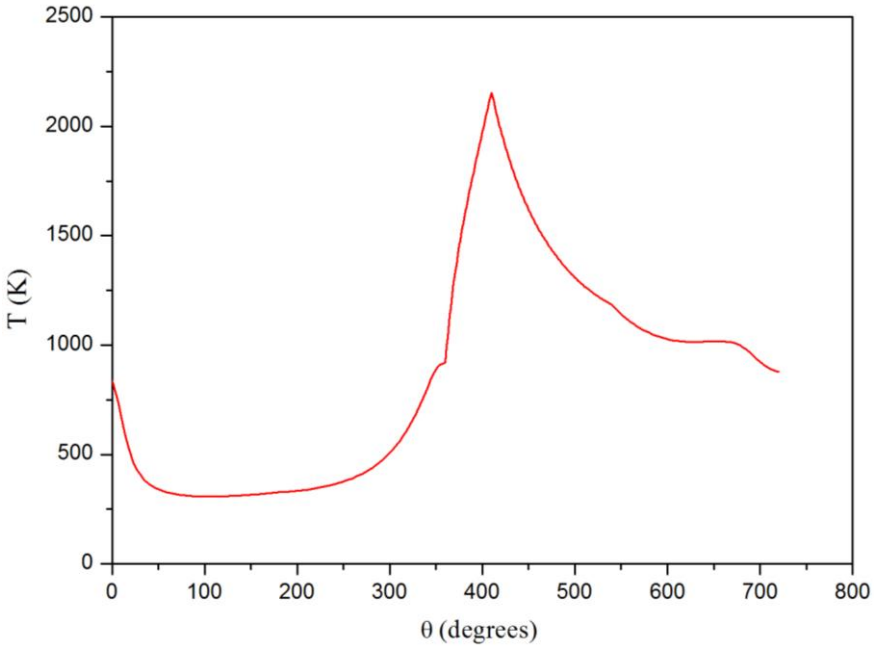


Figure 10. Lindec 4LD2500 T×θ @ 2800 rpm. Data from mathematical model simulation. From: author.

The irreversibility such as piston ring/cylinder friction, heat losses to the environmental, crankshaft bearing friction, drive power to fuel pump and camshaft and others are adjusted from experimental data taken from Pereira HR (2006).

The coefficients *C1* and *C2*, used to evaluate $\overline{P_{fr}}$ in Eq. (11), were obtained by trial and error using the mathematical model and comparing it with experimental data. The results are *C1* = 275000 N m$^{-2}$ and *C2* = -73 N m$^{-2}$ rpm$^{-1}$. EACE simulation is evaluated with the same equation and coefficients.

## 5. RESULTS AND DISCUSSIONS

A comparative between the IC-ICE Lindec 4LD2500 mathematical model and EACE is performed. The EACE simulation use the same volumetric displacement and others geometric characteristics and the same $AFR_{real}$.

From the simulated data are taken $\dot{W}\times rpm$ and $\eta\times rpm$ diagrams. Fig. 11 shows them. Note EACE curve shift, an improvement of 33 % in $\eta$. Figure 12 shows $T\times\theta$ diagram at 2800 rpm, note the peak temperature comparing with Fig. 10.

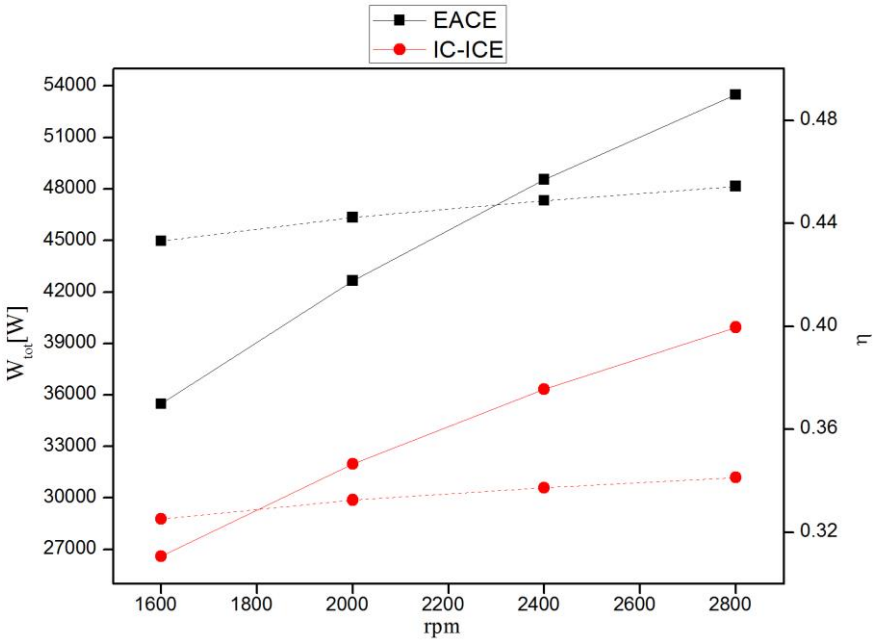


Figure 11. $\dot{W}_{tot}\times rpm$ and $\eta\times rpm$ comparative between IC-ICE and EACE. $\eta$ in dashed lines. Data from mathematical model simulation. From: author.

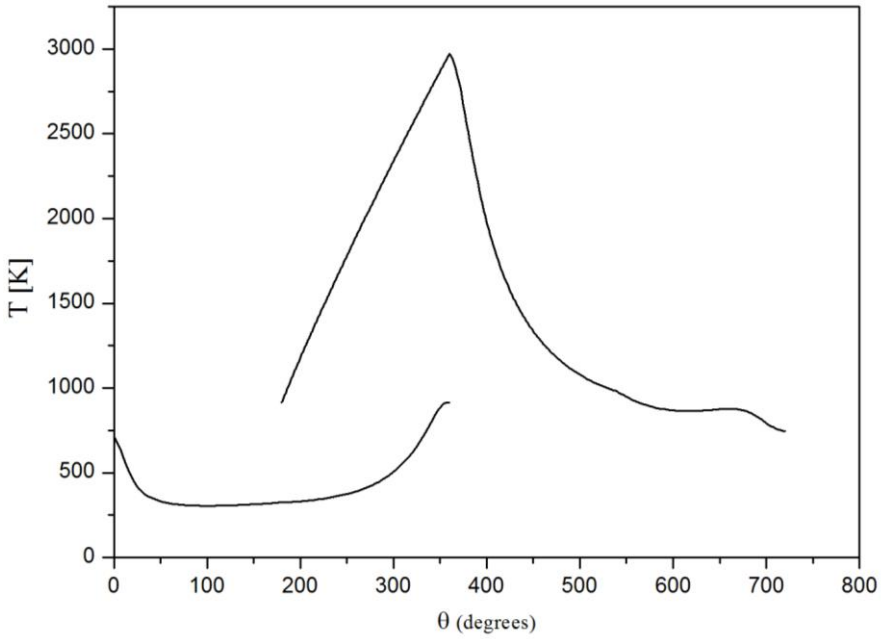


Figure 12. EACE $T \times \theta$ diagram. Data from mathematical model simulation. From: author.

Figure 13 shows the $P \times V$ comparative diagram between IC-ICE and EACE 2800 rpm. The area below the expansion curve less the area below the compression curve gives the work delivered by the cycle (not considering the admission exhaust process). Note that the EACE area is larger than IC-ICE area. Which shows graphically EACE cycle can deliver more useful work than the IC-ICE cycle for the same volumetric displacement and geometric characteristics and the same $AFR_{real}$. Additionally, it is important to observe the EACE compression and expansion strokes are very similar to the same strokes of the Stirling cycle shows in Fig. 3.

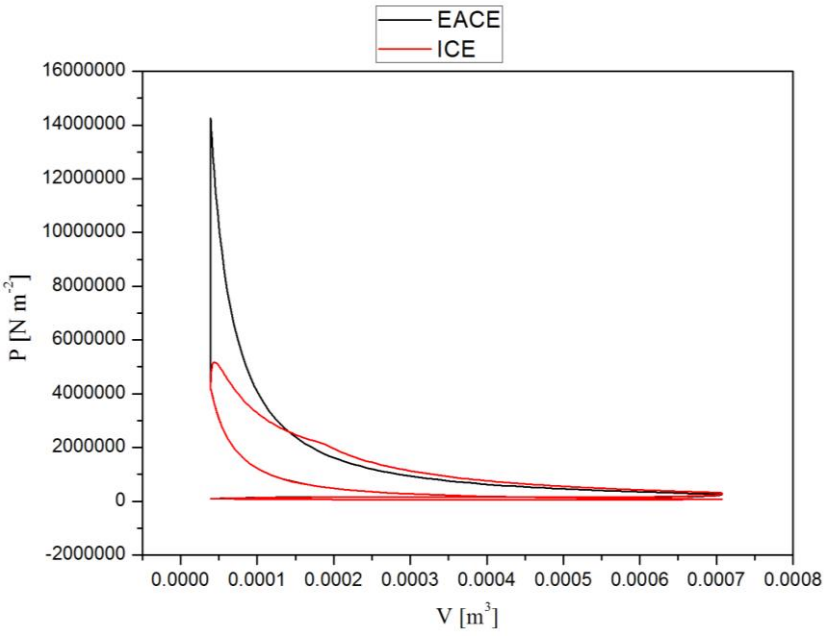


Figure 13. $P \times V$ diagram comparative between EACE and IC-ICE. Data from mathematical model simulation. From: author.

## 6. CONCLUSION

From the theoretical results, we can conclude that there is an approximately 33 % increase in the efficiency of the EACE when compared with an IC-ICE with the same volumetric displacement, same geometric characteristics, and same $AFR_{real}$. In all the speed range analyzed.

Combustion in an external chamber adds one-step to the operating cycle of the IC-ICE, the adiabatic combustion step. In this step, an isochoric compression occurs, without the need to supply work to the stage. This is one of the main reasons for the increasing cycle efficiency. In addition, since combustion occurs in a thermally insulated chamber, there is no heat loss at this stage, also contributing to improved efficiency.

Several new features need to be developed to become this engine feasible like the new kinematic mechanism, the connection of the cylinders with the external chamber, the new inlet and outlet valves arrangement, the new cylinder and piston cooling system, the expansion and compression process in separated cylinders and others. All these features need to be developed in futures studies.

A side effect, but also very important, that occurs with the inclusion of the adiabatic combustion step is the increase in the combustion time. This would allow the burning of heavier and more complex fuels. Such as biodiesel, heavy vegetable oils and even solid fuels.

Other very interesting possibilities are, as the expansion and compression process takes places in separated cylinders, the possibility to adjust different displacement volumes for each process to get the largest work possible from the working fluid, similar that occurs at Atkinson cycle.

## 7. ACKNOWLEDGEMENTS

The authors acknowledge with gratitude the research was supported by the National Council for Scientific and Technological Development, CNPq, Brazil.

## 8. REFERENCES

Adler, Jonas and Bandhauer, Todd, 2017. “Performance of a Diesel Engine at High Coolant Temperatures”. *Journal Of Energy Resources Technology*, [s.l.], v. 139, n. 6, p.062203-062203, 27 jun. 2017.

Graciano, Vilmar; Vargas, Jose Viriato C.; Ordonez, Juan C.,2015. “Modeling and simulation of diesel, biodiesel and biogas mixtures driven compression ignition internal combustion engines”. *International Journal Of Energy Research*, [s.l.], v. 40, n. 1, p.100-111, 23 jan. 2015.

Li, Tingting; Caton, Jerald A.; Jacobs, Timothy J., 2016. “Energy distributions in a diesel engine using low heat rejection (LHR) concepts”. *Energy Conversion And Management*, [s.l.], v. 130, p.14-24, dez. 2016.

Liu, Hanfeng et al., 2018. “Investigation on the Potential of High Efficiency for Internal Combustion Engines”. *Energies*, [s.l.], v. 11, n. 3, p.513-533, 27 fev. 2018. MDPI AG.

Moran, Michael; Shapiro, Howard, 2000. “Princípios de Termodinâmica para Engenharia”. 4. ed. New York: Wiley & Sons, Inc, 2000.

Pereira HR., 2006. “Experimental evaluation and performance prediction of diesel and natural gas driven diesel engines”. Doctoral dissertation. Pontifícia Universidade Católica do Rio de Janeiro, Brazil, 2006. (in Portuguese).

Santos, R.F.E.; Santos, A.M.; Martins, K.C.R.; Silva, J.A., 2004. “Análise de Detonação, Torque e Potência em um Motor de Ignição por Compressão Turbo-alimentado por um Sistema Ternário de Combustíveis – Diesel, Biodiesel e Etanol”. III Congresso Nacional de Engenharia Mecânica / CONEM; Belém, PA.

Thombare, D.g. and Verma, S.k., 2008. “Technological development in the Stirling cycle engines”. *Renewable and Sustainable Energy Reviews*, [s.l.], v. 12, n. 1, p.1-38, jan. 2008.

## 9. RESPONSIBILITY NOTICE

The authors are the only responsible for the printed material included in this paper.